Journal of Membrane Science & Research

journal homepage: www.msrjournal.com

Research Paper

On the Origin of the Membrane Potential Arising Across Densely Charged Ion Exchange Membranes: How Well Does the Teorell-Meyer-Sievers Theory Work?

A.H. Galama[1,2], J.W. Post[1], H.V.M. Hamelers[1], V.V. Nikonenko[3], P.M. Biesheuvel[*1,4]

[1]*Wetsus, European Centre of Excellence for Sustainable Water Technology, Oostergoweg 9, 8911 MA Leeuwarden, The Netherlands*
[2]*Sub-Department of Environmental Technology, Wageningen University, Bornse Weilanden 9, 6708 WG Wageningen, The Netherlands*
[3]*Membrane Institute, Kuban State University, 149 Stavropolskaya str., 350040 Krasnodar, Russia*
[4]*Laboratory of Physical Chemistry and Colloid Science, Wageningen University, Dreijenplein 6, 6703 HB Wageningen, The Netherlands*

ARTICLE INFO

Received 2014-11-03
Revised 2015-01-15
Accepted 2015-01-15
Available online 2015-01-15

KEYWORDS

Ion exchange membranes
Nernst-Planck equation
Donnan equilibrium
Teorell-Meyer-Sievers (TMS) theory

GRAPHICAL ABSTRACT

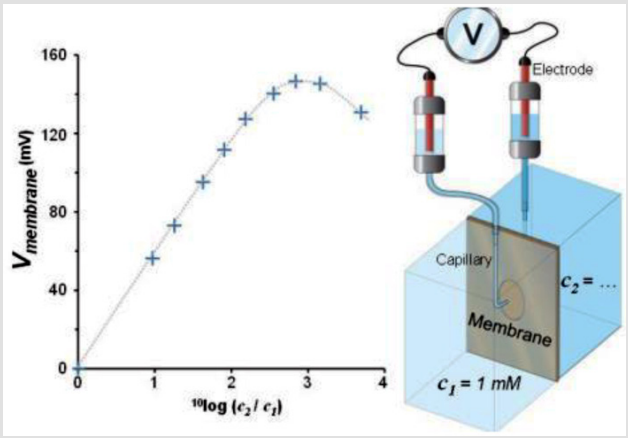

HIGHLIGHTS

- The origin of the membrane potential across ion exchange membranes (IEMs) is discussed
- At large concentration differences, Teorell-Meyer-Sievers (TMS) theory deviates from the data
- No single assumption in the TMS theory can by itself account for the deviation
- For highly charged IEMs the membrane potential can go through a maximum
- Presence of a maximum in the potential depends on the concentration ratio

ABSTRACT

A difference in salt concentration in two solutions separated by a membrane leads to an electrical potential difference across the membrane, also without applied current. A literature study is presented on proposed theories for the origin of this membrane potential (ϕ_m). The most well-known theoretical description is Teorell-Meyer-Sievers (TMS) theory, which we analyze and extend. Experimental data for ϕ_m were obtained using a cation exchange membrane (CMX, Neosepta) and NaCl solutions (salt concentration from 1 mM to 5 M). Deviations between theory and experiments are observed, especially at larger salt concentration differences across the membrane. At a certain salt concentration ratio, a maximum in ϕ_m is found, not predicted by the TMS theory. Before the maximum, TMS theory can be used as a good estimate of ϕ_m though it overestimates the actual value. To improve the theory, various corrections to TMS theory were considered: A) Using ion activities instead of ionic concentration in the external solutions leads to an improved prediction; B) Inhomogeneous distribution of the membrane fixed charge has no effect on ϕ_m; C) Consideration of stagnant diffusion layers on each side of the membrane can have a large effect on ϕ_m; D) Reducing the average value of the fixed membrane charge density can also largely affect ϕ_m; E) Allowing for water transport in the theory has a small effect; F) Considering differences in ionic mobility between co-ions and counterions in the membrane affects ϕ_m significantly. Modifications C) and F) may help to explain the observed maximum in ϕ_m.

1. Introduction

Whenever there is a salt concentration difference over the membranes of, for instance, an electrodialysis (ED) stack, an electrical potential (or voltage) can be measured. In the absence of a current, this membrane potential is also referred to as the open circuit voltage (OCV), the reversible potential, the concentration potential, or by the more general term of electromotive force (emf). This 'reversible' potential determines the minimum energy that is required to transport charge, as for example in the ED process [1]. Vice versa,

* Corresponding author at: Tel: +31 (0)58 284 3000, Fax: +31 (0)58 284 3001
E-mail address: maarten.biesheuvel@wetsus.nl (P.M. Biesheuvel)

it is also a measure of the maximum amount of energy that can be recovered in a process such as reversed electrodialysis [2,3], or during the energy recovery step in membrane capacitive deionization [4,5]. Recently the membrane potential of living cells was identified as a key indicator of normal cell growth, and changes in the membrane potential to be related to carcinogenesis [6-8].

The phenomenon of the membrane potential at zero current conditions is intriguing and has fascinated many scientists for more than a century. Already in 1890, Wilhelm Ostwald [9] sketched the situation of two electrolyte solutions separated by a semipermeable membrane and drew attention to the (electrical) effects in these kinds of systems. Two decades later (1911), Frederick Donnan described the equilibrium of ions between two phases, separated by a semipermeable membrane, of which one phase contains a fixed charge (non-permeating species) [10]. Both these works became very important in the development of theories to explain the membrane potential that arises over biological membranes or artificial ion exchange membranes (IEMs).

In our present work we discuss the assumptions underlying the theory for the membrane potential describing the phenomena occurring when a semipermeable membrane separates two electrolyte solutions differing in salt concentration. We will restrict ourselves in this work to theory and data applying to the situation where the electrical current is zero. The most fundamental and well-known theoretical approach to describe the membrane potential is the Teorell-Meyer-Sievers (TMS) theory [11,12]. Using this theory the membrane potential can be well predicted within certain ranges of the salt concentration. However, as we will show, for outside this range, the TMS theory markedly deviates from the experimental data. In the present work, we thoroughly analyze the TMS theory and develop various extensions of TMS theory to better describe experimental data for the membrane potential. We discuss in which way each extension influences the theoretical results.

2. Theory

In this section we describe the basic theory of ion transport in ion exchange membranes. We show how under zero current conditions a difference in chemical potential across an IEM induces the development of an electric potential difference. We first neglect a contribution by convection (due to water flow) on ion transport. The development of the TMS theory from the ion transport equations will be clearly described. Also the extension of the TMS theory to the Space Charge Model (SCM) will be discussed briefly.

2.1. Potentials and transport

Transport of ions through a membrane can take place by migration, diffusion and convection. Migration is the transport of ions caused by an electric potential gradient ($\nabla\phi$), diffusion is the movement of ions caused by a chemical potential gradient ($\nabla\mu$), and convection is the transport of ions due to a pressure gradient (∇P). These three different gradients act as driving forces for transport and simultaneously result in i) electrical current, ii) ionic flow, and iii) fluid flow [13-15]. These three fluxes are interrelated, and to predict the flux of a certain ionic species, all three forces acting on the ions should be taken into account simultaneously.

In the simplest 1:1 salt solution (e.g., NaCl) two ions are present and as such two electrochemical potential gradients should be considered. In solutions with many ionic species, e.g. seawater, the electrochemical potential can be calculated for all individual ionic species, as shown by Leyendekkers [16] and Whitfield [17]. Due to the combination of different gradients acting on the ions in solutions, it is not obvious what will be the direction and velocity of the ionic fluxes. Even without an applied electrical current and applied pressure, it is possible that ions are transported through the membrane against their own chemical potential gradient, a phenomenon known as uphill ion transport [15,18,19].

In the ED process [20,21], the largest driving force for transmembrane ionic transport is in most cases the applied electrical potential difference. In ED, a dilute and concentrate stream are formed. The concentration difference between these two streams can be large, and a large difference in chemical potential, $\Delta\mu$, can therefore arise during the process. This increasing $\Delta\mu$ results in an increasing driving force for ion transport in opposite direction to the electric driving force, which leads to a decrease of the ion flux. This decrease of the ion flux is sometimes referred to as "back diffusion" of ions. Convective ion transport through IEMs is usually assumed to be negligible and is often left out of the ion transport equations [22-24].

To describe ion transport, the chemical potential, μ_i (J/mol), and the electric potential, ϕ (V), are combined in the electrochemical potential, $\tilde{\mu}_i$ (J/mol), which is calculated as

$$\tilde{\mu}_i = \mu_i + z_i F\phi = \mu_i^0 + RT\ln c_i + z_i F\phi \tag{1}$$

where z_i is the ion valence (-), F the Faraday constant (C/mol), R the gas constant (J/mol K), T temperature (K), and c_i the ion concentration (mol/m^3=mM). For now, thermodynamic non-idealities are not discussed [25-27]. According to Donnan equilibrium, two phases in contact with each other eventually will have the same electrochemical potential [10,28]. The electric potential developing over an interface (with side L and side R) for a single solute solution can then be obtained according to the balance

$$\mu_i^0 + RT\ln c_i^L + z_i F\phi^L = \mu_i^0 + RT\ln c_i^R + z_i F\phi^R \tag{2}$$

which can be simplified to

$$RT\ln c_i^L = RT\ln c_i^R + z_i F(\phi^R - \phi^L) \tag{3}$$

and rewritten to

$$\Delta\phi = \phi^R - \phi^L = \frac{V_T}{z_i}\ln\left(\frac{c_i^L}{c_i^R}\right) \tag{3}$$

where V_T is the thermal voltage, defined as V_T=RT/F. Eq. (4) is the well-known Nernst equation (for general cases and for an electrode-solution interface), or Donnan relation (for a solution-membrane interface). This equation is often used to estimate the electric potential over the membrane in the absence of a current, as it gives the theoretically maximum membrane potential, ϕ_{max} [29,30]. In biological cells, an unbalanced situation between the internal and the external solution is often maintained by ion pumps, and the resulting membrane potential is then known as the resting membrane potential, also described by Eq. (4).

Eqs. (1)-(4) show that the measured electrical potential results from the electrochemical potential gradient, $\nabla\tilde{\mu}$, which is present in a defined system. When differentiating Eq. (1) in the transport direction, x (i.e. perpendicular to the membrane), this electrochemical potential gradient can be expressed as

$$\frac{\mathrm{d}\tilde{\mu}_i}{\mathrm{d}x} = RT\frac{\mathrm{d}\ln c_i}{\mathrm{d}x} + z_i F\frac{\mathrm{d}\phi}{\mathrm{d}x} \tag{5}$$

This gradient is the negative of the driving force on an ion, and results in an ion molar flux, J_i (mol/m^2 s), in solution and membrane. By definition a molar flux is the product of molar concentration and velocity. This velocity is the product of the mobility and the total driving force. Combined in one formula, the ionic flux is given by

$$J_i = -\frac{u_i}{F}c_i\frac{\mathrm{d}\tilde{\mu}_i}{\mathrm{d}x} \tag{6}$$

where u_i is the electric mobility (m^2/V s), which is related to the ion diffusion coefficient, D_i (m2/s) according to the Einstein(-Smoluchowski) relation [31,32]

$$D_i = u_i V_T \tag{7}$$

Inserting Eqs. (5) and (7) in Eq. (6) results in

$$J_i = -\frac{D_i}{RT}c_i\left(RT\frac{\mathrm{d}\ln c_i}{\mathrm{d}x} + z_i F\frac{\mathrm{d}\phi}{\mathrm{d}x}\right) \tag{8}$$

which is the well-known Nernst-Planck flux equation that can be rewritten to the more common form

$$J_i = -D_i\left(\frac{\mathrm{d}c_i}{\mathrm{d}x} + c_i\frac{z_i}{V_T}\frac{\mathrm{d}\phi}{\mathrm{d}x}\right) \tag{9}$$

In electrochemical system, the convective transport in the direction perpendicular to the membranes is often assumed to be negligible in comparison with the diffusion and migration terms [33-39]. Therefore a convective term, $c_i \cdot v_f$, where v_f is the fluid (water) velocity (m/s), has for now been neglected in Eq. (9). The fluid velocity results from pressure differences, ion concentrations and a water-membrane friction coefficient, $f_m\delta$ (mol s/m^4), see Eqs. (29) and (30) in reference [40].

When there are multiple permeating monovalent species, and especially in biological systems [41], the membrane potential (ϕ_m) is sometimes calculated using the Goldman-Hodgkin-Katz (GHK) voltage equation [34,42]. This equation takes the permeability of each permeating species into account. The GHK equation is given by

$$\phi_m / V_T = \ln\left(\sum_{i=1}^{N} P_i c_i^L + \sum_{j=1}^{M} P_j c_j^R\right) - \ln\left(\sum_{i=1}^{N} P_i c_i^R + \sum_{j=1}^{M} P_j c_j^L\right) \tag{10}$$

where

$$P_i = V_T u_i \beta_i / \delta_m \tag{11}$$

where P is the ion specific permeability (m/s), δ_m the membrane thickness (m), β the partition coefficient (-) between the membrane and solution (defined by the Donnan equilibrium on the solution-membrane interface), and N and M refer to the number of ionic species. The GHK equation, Eq. (10), can be derived from the Nernst-Planck (NP) flux equation, Eq. (9), as described in references [34,35,42]. When there is only one permeating monovalent ion present, the GHK reduces to the Nernst equation, Eq. (4).

2.2. The membrane potential in IEMs

IEMs contain a high concentration of fixed charges. These charges are due to ion exchange groups that are covalently bound to the membrane polymer structure. For anion exchange membranes (AEMs), quaternary ammonium groups can be used, while cation exchange membranes (CEMs) can be based on sulphonic acid groups [24,43]. For commercial IEMs the fixed membrane charge concentration, here denoted by X, can be around 5-6 M when defined per volume of aqueous phase in the membrane [44,45]. This fixed membrane charge can be regarded as a non-diffusible ionic species [46] and as such participates in the Donnan equilibrium. Ions in the external solution with a charge sign opposite to that of the fixed charge groups, are called counterions, and these ions readily enter the membrane. Ions with the same charge sign as the fixed membrane charge are called co-ions, and these ions enter the membrane only in small numbers. The large difference between the internal concentration of co- and counterions in the membrane is often referred to as Donnan exclusion, and it determines the selectivity of the membrane [46-50].

With a concentration difference over an IEM, or over a stagnant diffusion layer (SDL, a layer through which ions can migrate, but without tangential fluid flow or fluid mixing), a diffusion potential (ϕ_{diff}) develops due to differences in ionic mobility of the diffusing ions [48,49,51]. If one ionic species diffuses faster than the other ($D_+ \neq D_-$), this will results in a minute charge separation that leads to an electrical potential gradient, $\nabla\phi$ [49]. In an IEM, and with zero current, $\nabla\phi$ aids the co-ion, and retards the counterion. Integrated over the entire membrane interior, the resulting diffusion potential ϕ_{diff} (also known as the constrained liquid junction potential) is related to the concentration gradient in the membrane of all ionic species [52].

To calculate the diffusion potential, we must first of all consider local electroneutrality (EN) in the membrane. For a 1:1 solution, EN relates at every position the concentration of counterions and co-ions according to

$$\bar{c}_{counterion} - \bar{c}_{co-ion} + \omega X = 0 \tag{12}$$

The parameter ω indicates the charge sign of the fixed membrane charge (ω=-1 for CEMs, and ω=+1 for AEMs). The diffusion potential can then be obtained by solving the Nernst-Planck equation, Eq. (9), for both co-ions and counterions, and making use of the zero-current condition,

$$J_{counterion} - J_{co-ion} = 0 \tag{13}$$

as further treated in Appendix A. In the theoretical case of a 100% permselective membrane, no mobile co-ions are present in the membrane phase, but only counterions and fixed membrane charges. In that specific case, due to the electroneutrality condition [11], no diffusion can take place and the diffusion potential is zero.

According to Donnan equilibrium, across the membrane/solution interfaces, the electrochemical potential of each ion must be equal in the external and internal phase. When using Eq. (4), and replacing left and right side by external and internal phase, one finds that there can be a substantial difference between the electric potential in the external phase, ϕ_{ext}, and in the internal phase, ϕ_{in}. The difference is the Donnan potential, $\Delta\phi_D$, and relates to the electrical double layer (EDL) that forms at the membrane/solution interface [28,48]. Because there are two such interfaces, there are also two Donnan potentials, given by

$$\Delta\phi_D^L = \frac{V_T}{z_i}\ln\left(\frac{\bar{c}_i^L}{c_i^L}\right) \quad \text{and} \quad \Delta\phi_D^R = \frac{V_T}{z_i}\ln\left(\frac{\bar{c}_i^R}{c_i^R}\right) \tag{14}$$

Addition of these two Donnan potentials to the diffusion potential inside the membrane phase results in membrane potential, ϕ_m [22,33,44,49,53,60],

$$\phi_m = \Delta\phi_D^L - \Delta\phi_D^R + \phi_{diff} \tag{15}$$

where ϕ_m is the membrane potential (V), $\Delta\phi_D$ the Donnan potential (V) on the left hand (L) and right hand (R) side of the membrane, and ϕ_{diff} is the diffusion potential (V). Figure 1 shows these potentials schematically. The Donnan potential is also referred to as the exclusion potential as it can include both electrostatic (repulsion) and steric (size exclusion) effects [49]. For ionic solutions steric effects are much smaller than electrostatic effects and are not further discussed in this work.

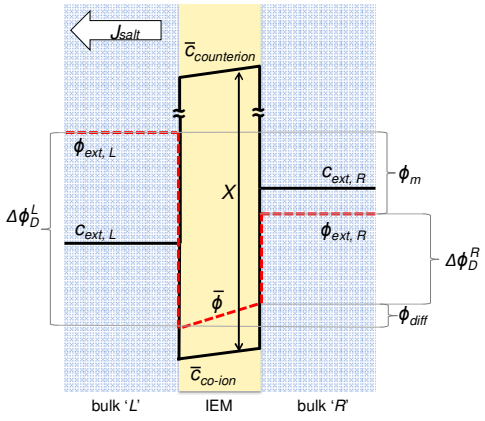

Fig. 1. Schematic representation of concentration, c, and potential, ϕ, profile in an ion exchange membrane (IEM) between two electrolyte phases of different concentration, bulk L and bulk R, when no current is applied. Here X is the fixed membrane charge, ϕ_{diff} the diffusion potential, $\Delta\phi_D$ the Donnan potential of side L or R, and ϕ_m is the resulting membrane potential.

2.2.1. Effect of the stagnant diffusion layer

With transport through the membrane, on either side of the membrane a stagnant diffusion layer (SDL) develops [15,22,23,25,61]. This layer, or film, is also known as the Nernst diffusion layer [22,62-64], diffusion layer [22,24] or (diffusion) boundary layer [23,43,48]. In the absence of current, diffusion initiates mass transport, and in case ions have different diffusion coefficients,

migration develops as a driving force upon the ionic species in an SDL, which results in a diffusion potential across the SDL. Therefore, Eq. (15) can be extended with the potentials arising over the SDLs adjacent to the membrane, and the total membrane potential is then [25,65-68]:

$$\phi_m = \phi_{diff}^{SDL,L} + \Delta\phi_D^L + \phi_{diff}^m - \Delta\phi_D^R + \phi_{diff}^{SDL,R} \tag{16}$$

as schematically shown in Figure 2.

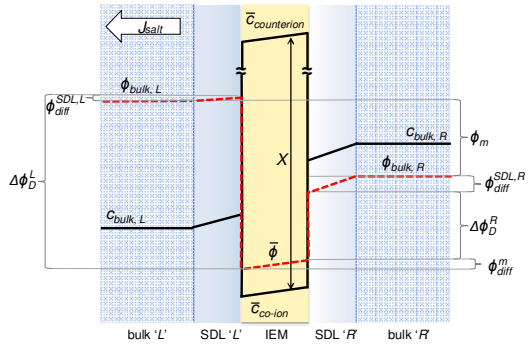

Fig. 2. Schematic representation of concentration, c, and potential, ϕ, profile in the bulk solutions, the stagnant diffusion layers (SDLs), and in an ion exchange membrane (IEM) when no current is applied. Symbols as in Figure 1.

Generally, the diffusion potentials due to transport across the SDLs are neglected when considering the membrane potential, which is justified at low concentration differences over the membrane, very thin SDLs, and densely charged IEMs. However, effects of the SDLs are often considered in processes where an electric potential is applied over one or multiple IEMs, such as in electrodialysis. In that case, when an electric current is applied over an IEM (and the accompanying SDLs), concentration polarization takes place in these SDLs [38,63,65,69]. Concentration polarization is then caused by the membrane selectivity between counterions and co-ions [24,43,48]. The diffusional and migrational forces acting on ions when a current is applied are schematically shown in Figure 3. So, besides formation of a diffusion potential in the SDL, concentration polarization in the SDL affects the ion concentrations at the membrane-solution interfaces, which also affects the membrane potential. The relative influence of the SDL depends on i) the ratio of SDL thickness, δ_{SDL}, over the membrane thickness, δ_m (m), ii) the ratio of the ion diffusion coefficient in the SDL, D over the ion diffusion coefficient in the membrane, $\bar{D}$ (m2/s), and iii) the ratio of the external ion concentration c, over the internal ion concentration $\bar{c}$ (mM) [22,25].

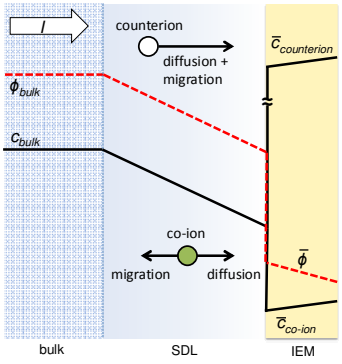

Fig. 3. Schematic representation of concentration, c, and potential, ϕ, profile in the bulk solution, the stagnant diffusion layer (SDL), and in an ion exchange membrane (IEM) when a current is applied. Driving forces acting on the ions are shown as vectors.

2.3. Modeling the IEM potential

The membrane potential across an IEM is widely studied, especially for situations were only monovalent ions are present [53,55,58,70-72]. A more limited number of studies discussed the membrane potential when the membrane is separating ionic mixtures with divalent ions [53,54,56,57,73,76] while for multi-ionic mixtures, the membrane potential is not often studied [53,76]. Prediction of membrane potentials with multi-ionic electrolytes of different concentrations or different ion valencies is complicated and mathematically complex [53,76].

The earlier mentioned GHK equation, Eq. (10), that is often used in relation to biological membranes, is in most cases not suitable for calculation of the membrane potentials across IEMs. Attempts were made to expand the GHK equation to incorporate effects of surface charge and divalent ions [18,41,77,78], but an adequate prediction of the membrane potential of IEMs with the GHK equation is difficult [23,41]. For IEMs, many models were developed in an attempt to model the membrane potential. Basically three approaches to investigate the membrane potential are widely used; i) the Teorell-Meyer-Sievers theory, ii) the (electrokinetic) space charge model (SCM), and iii) the theory of irreversible thermodynamics. Of these three, the first two most easily implement physical and chemical information. In the present work the focus is on TMS theory, but also the SCM will be discussed. For the theory of irreversible thermodynamics, see for instance references [13,14,52,79-82].

2.3.1. Teorell-Meyer-Sievers theory

Eq. (15) is the starting point of the Teorell-Meyer-Sievers (TMS) theory [11,12,23,83-86], which is used to predict the membrane potential across an IEM. An expression for the standard TMS theory, given by Eq. (17), is derived in Appendix A as

$$\phi_m / V_T = \omega \ln\frac{c_R}{c_L}\left[\frac{X+\sqrt{X^2+4c_L}}{X+\sqrt{X^2+4c_R}}\right] + \bar{U}\ln\left[\frac{-\bar{U}\omega X+\sqrt{X^2+4c_L}}{-\bar{U}\omega X+\sqrt{X^2+4c_R}}\right] \tag{17}$$

where

$$\bar{U} = \left(\bar{u}_+ - \bar{u}_-\right)/\left(\bar{u}_+ + \bar{u}_-\right) \tag{18}$$

In Eq. (17), the first term on the right hand side is the Donnan potential, while the second term is the diffusion potential. Similar results can be obtained with the equation defined in ref. [86]. However, Eq. (17) differs from the equation given by Lakshminarayanaiah [23] and Barragan et al. [87], as there a ω-term (or minus sign) in front of the Donnan part is missing (the diffusion part in those equations equals Eq. (17) for ω=-1, but for the Donnan part ω=+1 is implicitly assumed).

The TMS theory is often used, as it is a one dimensional (1D) model that is mathematically not very complicated. The original TMS theory assumes only gradients from one side to the other of the membrane, membrane pores substantially larger than the ion radius, an ideal solution of point ions (activity coefficients of the ions to be equal to unity, so a_i=c_i), no pressure-volume term (no convection), and an equal and evenly distributed membrane charge at all external concentrations [11,12,23,83,84,86]. And although the TMS theory can predict the reversible membrane potential (OCV) for certain external concentration ranges [23], also (large) deviations are reported [49,57,58,84,86-89]. In the TMS theory one of the three driving forces, the pressure gradient, is neglected. The TMS theory was extended with the convective water flow in the 'uniform potential model' [15,25,90-92].

2.3.2. The space charge model

The SCM, or capillary pore model, developed by Osterle and co-workers [93-95] is a two dimensional (2D) model that takes into account gradients both in the axial and radial direction. Also, fluid transport is included in this model [96]. In contrast to TMS theory, the SCM includes assumptions about the membrane structure. This is necessary because radial gradients within the membrane pores are taken in account. In the original SCM, parallel cylindrical pores are assumed with the fixed membrane charge uniformly distributed over the pore walls while ions are regarded as point charges.

In the SCM, the NP equation, extended with a convection term, is used to describe the ion and water fluxes through the membrane. The Navier-Stokes equation is used for the fluid velocity in the pore. The Poisson-Boltzmann (PB) equation is used to describe the ion and electrical distribution (in the EDL) within the pore. The SCM is based on the three earlier mentioned driving forces that determine the membrane potential: the electric potential

gradient: the chemical (osmotic) potential gradient, and the pressure gradient [93-95,97]. These three driving forces are not independent but are linked by three equations with each three terms and three coupling coefficients (K_{ij}). The resulting 9 coupling coefficients reduce to 6 by Onsager's reciprocal theorem (K_{ij}=K_{ji}) [98]. It was already mentioned that whenever a concentration gradient ($\nabla\mu$) is present in a (charged) membrane, this will lead to the development of an electric potential gradient ($\nabla\phi$). However, due to differences in concentration (or composition) of the external solutions there is as well a difference in osmotic pressure (Π) in these external solutions which leads to an effective pressure gradient (∇P). So even if no (hydrostatic or hydraulic) pressure is applied (P_{hyd}), effectively a pressure gradient is present in the membrane, resulting in fluid flow (osmosis) through the membrane pores. The effective pressure gradient in the membrane is defined as [40,86,99,100]:

$$\nabla P = \nabla P_{hyd} - \nabla\Pi \tag{19}$$

By this definition, movement of fluid against a hydrostatic pressure, toward location of higher osmotic pressure (e.g. in seawater reverse osmosis) can be understood.

2.3.3. Water transport

Across the membrane-solution interface (I) of a highly charged IEM the osmotic pressure ($\Delta\Pi^I$) suddenly changes, because the ion concentration changes from the concentration in the external solution to the value in the internal solution (within the membrane) over a distance of the order of a few times the Debye length [90]. As shown by refs. [40,90,101], the change in the osmotic pressure results in an equal change in the hydrostatic pressure across the solution-membrane interface ($\Delta\Pi^I$=$\Delta P_{hyd}{}^I$). The pressure increase from the bulk to the internal solution will be larger on the membrane side facing the lower external solution ion concentration, resulting in a pressure gradient in the membrane pore that pushes the fluid flow towards the high salt concentration (positive or normal osmosis) [15,40,90,101,102]. Besides the pressure gradient, also the electric potential gradient (electric field) in the pore is a driving force for osmosis [40,90,103,104]. This fluid transport which is induced by ion migration is known as electro-osmosis [24,105]. Finally, water can be 'bound' to ions in the primary hydration sphere [106-108] or dragged along in a secondary hydration sphere or as 'free' water [107-109], which can lead to large water transport numbers [105,109]. Membrane properties influence the amount of water that is transported by the ions and in general a small pore size and hydrophobicity, or a low water content of the membrane, limit water transport [108-111].

Electro-osmotic transport depends on ion fluxes and ion diffusion coefficients and is independent of osmotic pressure. Direction and velocity of the fluid flow may vary with different ionic mixtures as described in refs. [15,90,101,104], so just as the solute (ions) also the fluid (water) can be transported against its chemical potential gradient (anomalous osmosis). Neglecting convection in the SCM, or including convection in the TMS theory, was found to have for most cases only a small effect on the calculated membrane potential [49,84,112].

2.3.4. Radial concentration gradients

In the SCM besides axial ion gradients, also radial ion gradients in the membrane pore are considered. It was found that the assumption of a uniform distribution of ions across the pore diameter leads to an overestimation of the co-ion exclusion effect, which results in incorrect estimation of the ion fluxes and the membrane potential in the TMS approach [49,86]. In the limit when EDLs in the membrane pores are fully overlapped, gradients in the radial direction disappear, and differences between the SCM and TMS theory (with convection included) must vanish. The thickness of the EDL is roughly represented by the Debye length and is a function of the external concentration, c_{ext}, at the membrane-solution interface [49,97]. At room temperature and for a monovalent 1:1 salt, the Debye length, λ_D (nm) can be approximated by $\lambda_D \approx 10/\sqrt{c_{ext}}$ (λ_D in nm, c_{ext} in mM) [113]. It should be noted that the Debye length is not based on the ion concentration within the EDL but on the concentration of the external solution [113]. For densely charged IEMs a typical pore radius, r_p, of ~1-2 nm may be assumed [43,86]. Thus, for c_{ext} = 10 mM, and $\lambda_D \approx 3$ nm, assuming fully overlapped EDLs is valid. However, at higher external concentrations, where $\lambda_D < r_p$, the assumption of fully overlapping EDLs would not be correct [114,115]. Radii of hydrated ions are several Ångström [116,117], so in densely charged IEMs, with nanoscopic pores, the volume fraction of ions in the pore is not insignificant [44,118]. Therefore, ions cannot be infinitely close to the wall, or to each other, and both the TMS theory, and the SCM (both of which assume ions as point charges) will overestimate the concentration of ions in the membrane pore [44, 86]. Also the thickness of the EDL will be influenced when the ion size is included, and will be larger than calculated with the PB equation. Fully overlapping EDLs may therefore be present at higher c_{ext} than estimated on the basis of the earlier given Debye length approximation. Detailed consideration of concentration profiles [119-121] will therefore be of less importance in very narrow and highly charged pores (r_p ~1-2 nm) where radial gradients diminish.

For membranes with larger r_p (e.g. used in nanofiltration, NF) and a considerable fixed charge density, these gradients are more important However, for membranes with large r_p and low fixed charge density, the gradient is also of less importance and predictions of the membrane potential by the TMS theory and the SCM will become closer again. Interesting are the cases with a low external concentration on one side and a high concentration on the other side of the membrane. In this situation, the EDLs can change from (fully) overlapping to (partly) non-overlapping along the axial direction. Proper estimation of the internal ion concentration is in that case required. Figure 4 gives a schematic representation of the concentration gradients in membrane pores according to the TMS theory and the SCM.

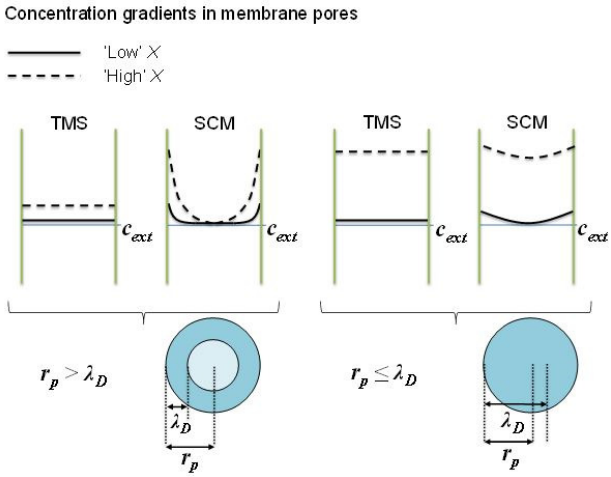

Fig. 4. Schematic representation of a membrane pore and the concentration gradients in the radial direction according to the theory of Teorell-Meyer-Sievers (TMS) and the space charge model (SCM). The solid line refer to membranes with a relative low fixed charge density, X, and the dashed lines to a membrane with a high fixed charge density. The external salt concentration, c_{ext}, is indicated by the thin line, pore radius is shown as r_p and the Debye length is λ_D.

To overcome some of the shortcomings of the SCM, Basu and Sharma [122] and Cervera et al. [86,118] extended the SCM theory and included effects of ion size, dielectric saturation, hydration, and surface charge regulation. By incorporating finite ion size the ionic selectivity increases, while on the other hand conductance will decrease as a result of lower internal concentrations and decreased diffusion coefficients [118,122]. Charge regulation, dielectric saturation and ion hydration significantly influence the model results and a good agreement with experimental results was obtained [122]. The effects of finite ion size and hydrodynamic retardation only became important for small pore diameters and high salt concentrations [122], e.g., for dense and highly charged IEMs.

3. Experimental section

3.1. Materials

The membrane potential over a CEM was experimentally investigated in a six-compartment stack, of which the details are described in refs. [123,124]. Two shields (Perspex 2 mm), with a circular hole were placed on either side of the membrane under investigation. These shields lowered the effective area

of the membrane under investigation to 2.84 cm^2, instead of its standard effective area of 23.8 cm^2. These shields stabilize the membrane and lower the diffusion area between the measuring solutions. All membranes in the setup are CEMs (CMX, Neosepta®, Tokuyama Corporation, Japan). The effective area of the four auxiliary membranes was 23.8 cm^2 each, and all six compartments had a volume of 95 mL.

A galvanostat (Ivium Technologies, The Netherlands) was used to measure the electrical potential over the membrane under investigation. To measure this potential, two Haber-Luggin capillaries were placed on either side of the membrane. These capillaries were connected with a reservoir by silicon tubes (inner diameter 4 mm, length ~100 mm). Both reservoir and capillary were filled with the same solution (and same concentration) as present in the specific compartment. In these reservoirs Ag/AgCl gel electrodes (QM711X, QIS, The Netherlands) were placed, which were connected to the galvanostat. The distance between the capillary tip and the membrane was 4.5±0.1 mm and was equal for all measurements. Salt solutions were prepared with demineralized water and NaCl (analytical grade, Boom B.V., The Netherlands). The concentrations of the measurement solutions were varied between 0.01-1.1 M in the first series of experiments, also described in ref. [124] and shown in Figure 5. For the second series experiments (results are shown in Figure 8) the solution concentration was in the range of 0.001–5 M.

3.2. Methods

Using a thermostatic bath the temperature of the solutions in the six-compartment stack was controlled at 25 ± 0.5 °C. The solutions were kept in 1 L bottles, which were submerged for 75% in the thermostatic bath. Solutions were circulated through the stack with a flow rate of 170 mL/min. Before start of each experiment the temperature was checked with a glass thermometer.

The membranes under investigation were stored in a 0.5 M NaCl solution. After installing the membranes in the stack, they were equilibrated for at least 1 hr with the measurement solutions on each side of the membrane before the experiment was started. After this time, solutions in the system were refreshed and continuously flushed through the stack in order to undo possible concentration changes in the solution due to diffusion effects. The largest concentration gradient over the membrane was present when solutions of 1 mM and 5 M were used. The difference in conductivity of these two solutions was measured directly before and after the experiment. The change in conductivity was always <1%. Therefore, concentrations of the solutions could be considered constant during the experiments.

The membrane potential was measured under open circuit conditions (1 measurement/sec) by chronopotentiometry [124]. Three series of measurements were made. Each series started with 5 min open circuit conditions, followed by a defined range of applied current densities [124]. The first minute after applying the current was not used for measuring the membrane potential. Based on the remaining (3x) 4 min, the average membrane potential was determined. The same measurements were also made with the salt concentration gradient reversed, i.e., the solutions on either side of the membrane were switched around. A second, independent measurement value of the membrane potential was thereby obtained. When there is no concentration difference over the membrane, the membrane potential is by definition zero. However, due to offset between the two reference electrodes still a potential can be measured. This offset was determined as 1.4±0.1 mV. The experimentally determined values were corrected for this electrode offset.

4. Results & Discussion

4.1. Experimental results

Figure 5 shows the experimentally determined, and theoretically calculated, membrane potential for different NaCl concentrations of the two external solutions (c_{low} and c_{high}).

When the two external solutions are equal (c_{low}=c_{high}), there is no gradient in any property and consequently there is no membrane potential (as $\nabla\phi = \nabla P = \nabla\mu = 0$). For c_{low}≥0.3 M, Figure 5 shows that the experimental and theoretical potentials are very close. However, when c_{low}=0.1 M, a small, but distinct, difference develops between the experimental and theoretical value of ϕ_m, and the deviation of TMS theory increases when c_{low}=0.01 M. The TMS theory, Eq. (17), overestimates the experimentally obtained membrane potential. This overestimation of the membrane potential was also reported in references [23,49,57,87,88,125]. These deviations imply that certain assumptions in the TMS theory are no longer valid for the dense and highly charged CMX membranes which are used here, under the experimental conditions.

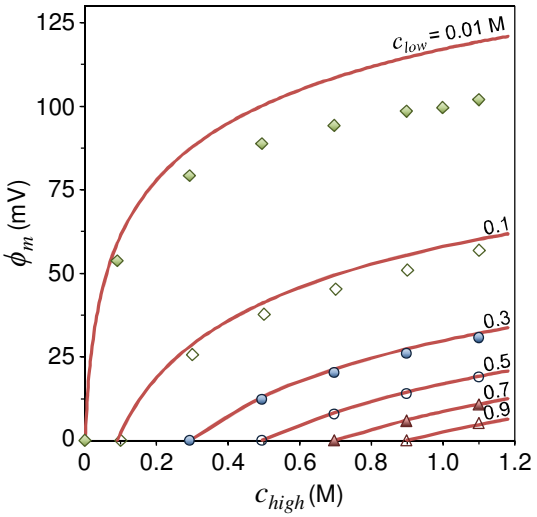

Fig. 5. Measurement of the membrane potential (ϕ_m, mV) as function of low and high salt concentration (c_{low} next to lines; c_{high} plotted on x-axis). Solid lines: standard TMS theory.

The assumptions that are made in the TMS theory are as follows: i) No concentration gradient in the radial direction in the membrane pores; ii) Membrane pores are substantially larger than the ion radius; iii) Ions behave as thermodynamically ideal point charges (so a_i=c_i); iv) Membrane pores are homogeneous throughout the membrane, and the fixed membrane charge is evenly distributed; v) At the membrane surfaces Donnan equilibrium is established; vi) The membrane structure does not change, the pore volume is constant, and the membrane charge density is equal at all external concentrations; vii) Convective water transport is negligible; and viii) The ion mobility ratio in the membrane is equal to that in the external solution.

Assumptions i) and ii) from this list are considered valid for the dense and highly charged IEM used in the experiments. These assumptions were already discussed in section 2.3.4. The effect of the other assumptions (iii-viii) on the calculated membrane potential is investigated in the next section, where various modifications or extensions of the TMS theory are considered.

4.2. Theoretical results

Figure 6 shows in panels A–F how different parameters, which relate to assumptions iii)–viii) above, influence the predicted membrane potential according to the TMS theory. The different panels show the effect of: A) ion activity, B) inhomogeneous distribution of the fixed membrane charge, C) including SDLs in the TMS theory, D) assuming a decreased (effective) membrane charge density, E) including osmotic water transport, and F) changing the ion mobility ratio. Concentration c_{low} was fixed at 0.01 M, while c_{high} is indicated on the x-axis. Solid lines give the standard TMS theory, and dashed lines are for modifications of the model.

Figure 6-A shows the effect on the TMS theory when the ion concentrations of the external solutions are replaced by the ion activities that are calculated according to

$$a_i = \gamma_i c_i \tag{20}$$

where a_i is the ion activity (mM) and γ_i the ion activity coefficient (-). To support the use of Eq. (20) we must note that not all solutions that we used were dilute, so that γ_i=1 is not a valid in all cases [23,84]. The activity coefficients were obtained from ref. [126]. Figure 6-A shows the quite significant difference between the TMS theory based on concentrations, and the modified approach using activities. In addition, we compare in Figure 7-A TMS theory with the maximum, Nernst, membrane potential (ϕ_{max}) according

to the Donnan relation (Eq. 4), which is very close to TMS theory. This implies that the effect of the diffusion potential ϕ_{diff}, on the membrane potential, ϕ_m, is very small, which is expected because $X>>c_{ext}$. This also implies that in this case, activity coefficients in the membrane can be neglected. For that reason as a first approximation we can simply replace in the TMS theory the ion concentrations in the external solutions by the ion activities which then affects the Donnan potentials [86]. Use of ion activities greatly improves the prediction of the membrane potential when c_{high}=0.1-0.3 M, where the value of γ changes, rapidly. In absolute terms, the effect is the largest when the activity coefficient reaches a minimum (at ~1 M). The effect of using ion activity instead of ion concentration diminishes when the concentration gradient is small and $\gamma_i^L \approx \gamma_i^R$.

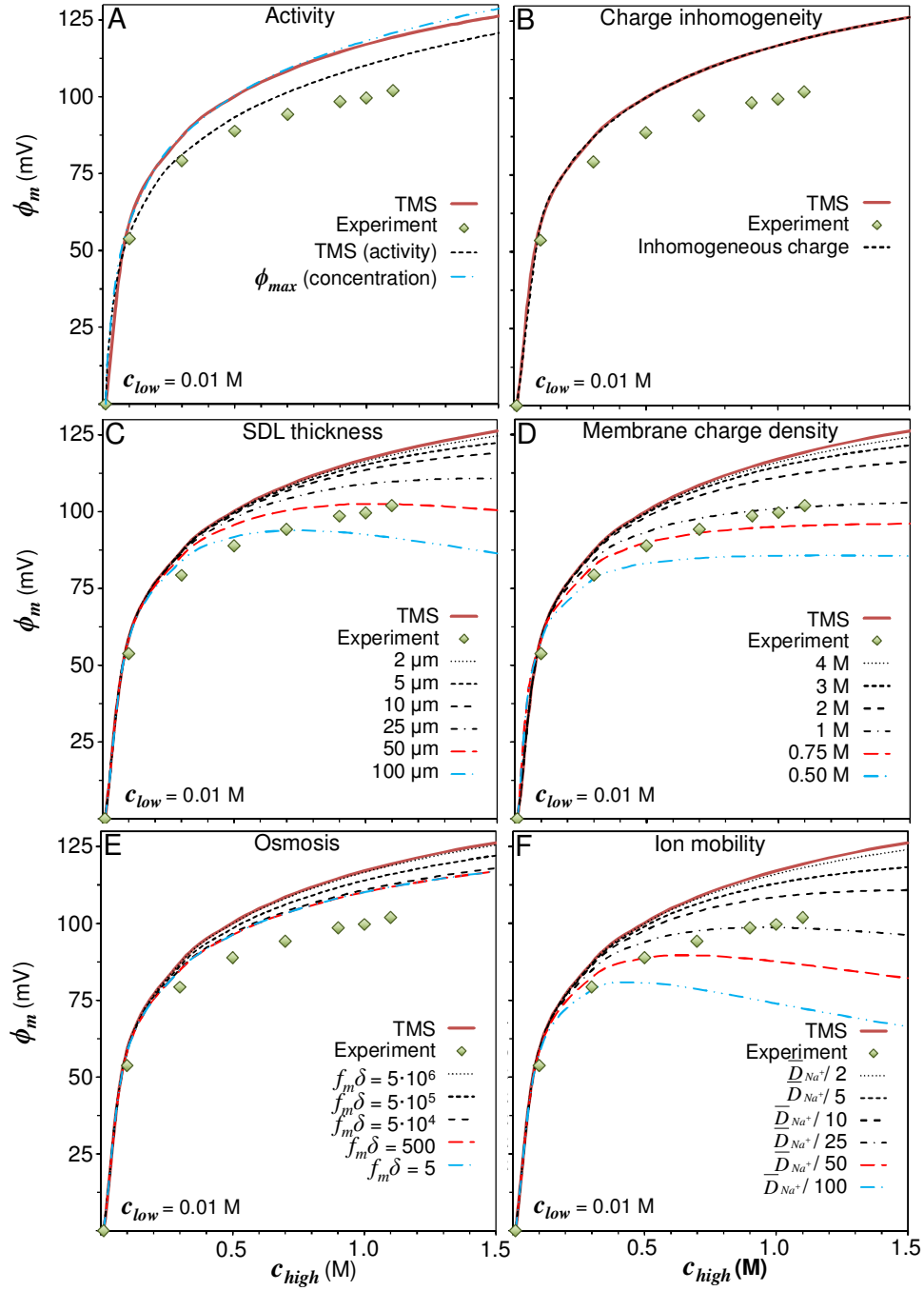

Fig. 6. Testing of six modifications of TMS theory. Diamonds: experimental values of membrane potential (ϕ_m, mV). Low external NaCl solution concentration 0.01 M; high concentration plotted on the *x*-axis. Solid line: standard TMS theory. Effect of A) Ion activity (activity coefficients in ref. [126]); B) Inhomogeneous charge distribution; C) Stagnant diffusion layers adjacent to the membrane of specified thickness (δ_{SDL}); D) Lowering the fixed membrane charge density; E) Osmosis at different water-membrane friction coefficients, $f_m\delta$; F) Lowering the diffusion coefficient of the counterion ($\overline{D}_{Na+}$) in the membrane.

In literature, activity coefficients of ions in the membrane and their effects on the membrane potential are discussed for instance in references [23,26,60,85,86,125,127-130], and also ion size effects, as observed in a previous work [44], can be included in this membrane activity coefficient [86]. However, activity coefficients in the membrane are unknown [129] and therefore, its usefulness for highly charged membranes is still a question [26].

Figure 6-B shows that the membrane potential is not affected by a possible inhomogeneous distribution of the membrane charge, X. An inhomogeneous distribution of charge from one side to the other side of the membrane can be due to the manufacturing process [131] or due to unequal swelling of the two membrane sides because of the different salt concentration. Ramirez et al. [131] showed different options of the spatial charge distributions, of which in this work only the influence of the most straightforward distributions will be investigated, namely i) an asymmetrical linear distribution, and ii) a symmetrical linear distribution. These two distributions are sketched in Figure 7. X was previously determined as ~5.7 M for the membranes that we use [44], and therefore this value is used as the average fixed membrane charge density (indicated as $\langle X \rangle$) in all cases.

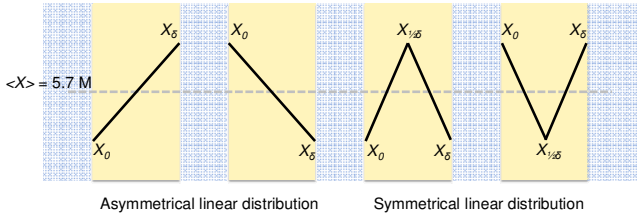

Fig. 7. Asymmetrical and symmetrical linear distribution of the fixed membrane charge X (M), where $\langle X \rangle$ is the average membrane charge density.

With the asymmetrical fixed charge distribution, there is a gradient in X across the membrane from position 0 to δ (left and right sides of the membrane). At one side the charge is lowered, on the other side the charge is increased relative to $\langle X \rangle$. With the symmetrical linear charge distribution, X is equal at both membrane-solution interfaces ($X_0 = X_\delta$), but these values are respectively above or below $\langle X \rangle$.

In the theoretical calculations performed for the present study, using a modified TMS theory including the unequal charge distribution, based on numerically solving Eq. (17), no effect of the charge distribution was observed. Small deviations (<1 mV) were found due to the numerical procedure, especially when there is a large gradient of fixed charge. Effect of an inhomogeneous distribution of the fixed membrane charge on the membrane potential was also studied in refs. [131-136]. It was suggested by data in refs. [133,136] that when membranes with an asymmetrical fixed charge distribution separate two solutions of equal composition, and no current is applied, the membrane potential is not zero ($\phi_m \neq 0$). However, according to our theoretical calculations this outcome is not possible, as was already discussed in the early 1970s in refs. [134,135]. These works conclude that such a potential can only be observed when no ions can penetrate the membrane, otherwise an internal diffusion potential will arise equal in magnitude, but of reversed direction as the difference in Donnan potentials [135]. In ref. [132] it is mathematically proven that under zero-current conditions, regardless of the fixed membrane charge distribution of an IEM, the membrane potential and salt transport must be zero when the membrane is separating two identical external solutions. In approximate models, non-zero equilibrium potentials can for instance arise due to invalidity of the Henderson equation [132]. This Henderson assumption is only valid when the external ion concentration is at least one order of magnitude smaller than the internal ion concentration ($c_{ext} \ll X$) [27,127,132].

When a current is applied over a membrane with a distribution of membrane charge, effects of the fixed charge distribution can be observed as described in refs. [131,137]. Whereas, the permselectivity is mainly determined by $\langle X \rangle$, other transport properties such as the selectivity can be observed to depend on the current direction in an asymmetrical membrane [131,137].

Figure 6-C shows the effect of including two SDLs (as shown by Eq. (16) and Figure 2) in the TMS theory (based on Eq. (15) and Figure 1). By including SDLs, assumption v) is affected, as the ion concentrations on the solution-membrane interface will change. Including SDLs in the model therefore lowers the theoretical membrane potential. The effect increases with SDL thickness, δ_{SDL}, as was also experimentally confirmed in ref. [68]. When an SDL thickness δ_{SDL} of 50 or 100 µm is used, the membrane potential shows a maximum. However, the shape of the curves differs significantly from the experimental data. Therefore, the simple addition of SDLs to the theory does not fully explain the observed differences between experimental and theoretical membrane potentials.

Figure 6-D shows the effect of the fixed membrane charge density on the membrane potential. As mentioned, X was determined as ~5.7 M per unit aqueous volume in the membrane [44]. Reference [44] showed that X slightly increases with increased external solution concentration. An increase of X, however, leads to a higher membrane potential, as directly follows from Eq. (17). In literature, it is sometimes assumed that the effective fixed membrane charge density, X_{eff}, is lower than the actual value of X [87,88,125]. The effect on the calculated membrane potential can be large when X is lowered substantially. However, this leads to the situation that X is no longer much larger than the external salt concentration. Barragán et al. [87,88] found similar differences between practical and theoretical membrane potentials as in the present work. They explained these differences by assuming that X_{eff} is lower than the actual membrane charge due to tight binding of counterions to the fixed membrane charge sites, as described in ref. [125]. However, in the present work, we argue that the effective membrane charge is equal to the actual membrane charge, at least as long as only NaCl is used as the salt. The ions Na^+ and Cl^- do not bind to the fixed charges sites [22]. Figure 6-D shows that a lower X results in a reduced membrane potential but this does not lead to a better description of the experimental data. It was shown in literature that with a further increase of c_{high} eventually membrane potentials will go down again [88,138]. This maximum in the membrane potential will be discussed later on.

Figure 6-E shows that adding water transport to the TMS equation [15,25,90-92] (i.e. adding the $+c_i \cdot v_f$ term to Eq. (9) and solving the model numerically) lowers the theoretical membrane potential. The water velocity, v_f, is a function of the concentration difference over the membrane, the ion fluxes, and a specified friction coefficient between membrane and water, $f_m\delta$ [40], as mentioned in the theory section. The water velocity is maximized at the highest concentration differences over the membrane (largest osmotic pressure difference) and for a minimum friction with the membrane, and is in opposite direction to the ion flux. In the standard TMS theory there is no water flow. When water flow with a high friction coefficient ($f_m\delta$ = 5×106 mol s/m^4) is included, the water velocity in the membrane is low and comparable to the counterion velocity (both in the order of 10 nm/s at a concentration difference of 0.01 vs. 1 M). In the membrane the water velocity is constant because the ions are assumed to have no volume in the Nernst-Planck equation. The ion velocity, however, depends on the local ion concentration (as the ion flux, $v \cdot c$, across the membrane is constant). The counterion concentration is almost constant throughout the membrane and thus the counterion velocity may be considered everywhere the same in the membrane. For co-ions, however, the concentration is strongly related to the ion concentration in the external solution [44] and, therefore, the ion velocity can be much higher at the membrane side that is facing the lowest external concentration (i.e. ~10,000 times higher at a concentration difference (0.01-1 M). When the water-membrane friction coefficient is lowered ten times ($f_m\delta = 5\times10^5$), this results in an increase of the water velocity (~6 times higher) and a slight decrease of the ion flux. Now the water velocity (~100 nm/s) becomes substantially higher than the counterion velocity, but is still much lower than the velocity of the co-ions. When the friction coefficient is lowered another ten times ($f_m\delta = 5\times10^4$), this only leads to a doubling of the water velocity to ~200 nm/s (at the concentration difference of 0.01-1 M). A further decrease of the friction coefficient does not lead to substantial higher water velocities, and the additive effect on the water flux diminishes. Thus the effect of water transport by itself seems too small to explain the deviation that is observed between experiment and theory, even when there is assumed (almost) no friction between water and membrane.

Earlier investigations on the effect of water transport on the membrane potential led to similar conclusions [49,60,84,112]. Sollner argues that measurement of correct stable potentials can be done long before any significant movement of water occurs [29], which underpins

the conclusion that water flow cannot be the origin of the discrepancy between data and theory.

Figure 6-F shows the effect of a difference in the ratio of mobility (or diffusion coefficient) of the counterion versus co-ion in the membrane compared to solution. In this calculation the ion mobility of the counterion is lowered to a greater extent when moving into the membrane, than for the co-ion. Usually it is assumed that the ionic mobility (of monovalent ions) in the membrane is around one order of magnitude smaller than the ionic mobility in the external solution, and that the ionic mobility ratio of counterions over co-ions is equal in the membrane and external solution (both ions are retarded in the membrane to the same extent). It is, however, unknown to what extent individual counterion and co-ion mobilities are different between the external and internal solutions. Thus, it is rather difficult to say what will be the sign of the diffusion potential across the membrane. As Figure 7-F shows, changing the ion mobility ratio has a direct effect on the membrane potential as shown also by Eqs. (17) and (18). The origin of a lower ionic mobility can be enhanced ion-ion, ion-membrane, or ion-fluid interaction [49]. As shown in Figure 6-F, the membrane potential decreases when the mobility of the counterion is lowered relative to that of the co-ion. The effect is very similar to the effect shown in Figure 6-C, which can be explained by the fact that in both cases the transport of the counterion becomes more restricted than the co-ion.

To conclude, the effects of the parameters shown in Figure 6-A to F do not (each by itself) explain the difference between experimental and theoretical membrane potentials that are shown in Figure 5. So, until now the TMS theory and the discussed modifications cannot explain the experimental results shown in Figure 6. It is most likely that a combination of the presented variables must be considered to explain the discrepancy between experiment and theory. With six variables to play with it seems certainly possible to fit the model to the experimental data in several ways [139], although the physical soundness of the different fitting parameters should then be carefully examined. The effect of each parameter will then be difficult to isolate [128] because the fitting parameters in the model affect each other (e.g. using activities leads to a lowered theoretical driving force for osmotic water transport). Isolation of effects of different parameters may only be possible with very precise experiments.

4.3. Maximum membrane potential

The experimental data in Figure 5 show that the membrane potential increases with an increasing concentration difference, Δc, of the two external solutions, c_{low} and c_{high}. This increasing membrane potential, however, seems to level off to a certain maximum value. Such a maximum value in membrane potential was also observed previously in references [88,138,140-143]. Beyond the maximum, the membrane potential decreases again. An 'ideal' membrane with perfect selectivity will have exactly the Nernst potential of Eq. (4). In that ideal membrane case there would be no maximum potential, but the potential infinitely increases with increasing Δc. To further investigate this interesting phenomenon of the leveling-off of the membrane potential, additional experiments were performed according to the same methodology as the experiments of section 4.1. The salt concentration on the low concentration side, c_{low} was either 0.001 M or 0.01 M NaCl, and c_{high} was between c_{low} and 5 M NaCl (0.001, 0.01, 0.02, 0.05, 0.1, 0.2, 0.5, 1, 2, or 5 M). Resulting membrane potentials from these experiments and the theoretical maximum potential, Eq. (4), are shown in Figure 8. To be consistent with ref. [138], the x-axis presents the activity ratio instead of the concentration ratio of the two external solutions.

Figure 8 shows for the CEM a perfect cation selective behavior, up to a ratio of external activities of ~100 ("log 2"). Beyond that, the membrane potential starts to deviate from the ideal Nernst potential, which can be explained by the decrease of membrane selectivity [23,138,142,143]. With c_{low}=0.01 M, we do not measure a maximum in the membrane potential, not even with c_{high}=5 M. However, when c_{low} is decreased to 0.001 M, a maximum in the membrane potential is observed, around c_{high}≈1-2 M NaCl. For even higher salinities the membrane potential decreases again, as was also observed in refs. [138,142]. The question is what the mechanism behind this decreasing membrane potential is when Δc becomes very large. In literature it was shown that a decrease in pore diameter and an increase in the fixed charge density postponed the deviation of the ideal potential (and formation of a maximum potential) to a larger external concentration ratio [138,142]. It was also suggested [142,143] that if the concentration of the external solution is similar to, or larger than, the fixed membrane charge density, the membrane loses its permselectivity, which then leads to a decrease in membrane potential.

However, in a previous investigation it was found that the fixed membrane charge density of the membrane is ~5.7 M [44], a concentration that was not reached in the experiments of Figure 8, but still a decrease was observed. Figure 8 furthermore shows that when c_{low} is increased from 0.001 to 0.01 M, the maximum in membrane potential is not found anymore. Moreover, when in that case c_{high} is 1 M (10log (a_{high}/a_{low}) ≈ 1.9) the membrane potential is still very close to the Nernst potential, while if c_{low} = 0.001 M and c_{high} = 1 M (^{10}log (a_{high}/a_{low})≈2.8) a much large deviation of the Nernst potential is observed. From these observations it can already be concluded that not only the value of the highest external concentration is important, but also the ratio of the low and high salt concentration.

The experimental results reported in Figure 9 suggest that the diffusive ion flux (of counterions and co-ions) through the pores is of influence to the membrane potential, as is also recognized by Makra et al. [142]. At the solution-membrane interfaces 'large' ion fluxes can cause concentration polarization. Figure 6 shows that including concentration polarization layers in the theory can help to explain the maximum in the membrane potential. Also further restriction of the counterion mobility compared to the co-ion mobility in the membrane can lead to the observation of a maximum membrane potential.

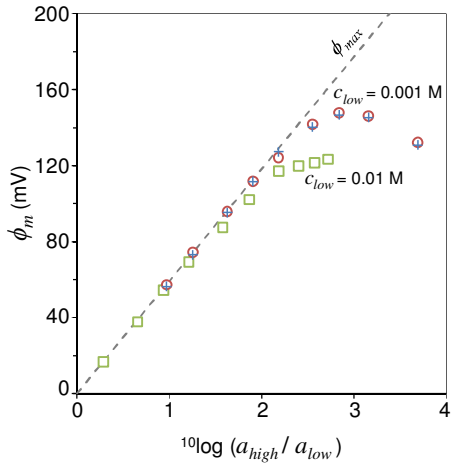

Fig. 8. Experimental membrane potential, ϕ_m, as a function of the logarithm of the ratio of the activity of the external solution with the high NaCl concentration, a_{high}, over the activity of the external solution with the low NaCl concentration, a_{low}. The dashed line indicates the activity based maximum potential, ϕ_{max}, according to Eqs. (4) and (20); c_{low} either 0.001 M (circles, crosses) or 0.01 M (squares), and c_{high} is varied between c_{low} and 5 M.

Note that in our work only three driving forces were considered, but it should be kept in mind that also a temperature difference, ΔT, can act as a driving force for mass transport [144,145]. This driving force becomes important in membranes used in fuel cell technology and membrane distillation [145,146]. Direction of the water flux due to temperature differences depends on the hydrophobicity of the membrane. Through hydrophilic membrane pores water is transported from the cold side to the hot side, while in a membrane with hydrophobic pores water is transported in the opposite direction [145,146]. Because in most membrane systems there is no, or only a very small, temperature difference between the external solutions, this driving force is neglected in most theories, although in electrochemical systems significant temperature gradients can locally be found [147].

5. Conclusions

With respect to the title question: 'How well does the Teorell-Meyer-Sievers theory work?', the answer is that for the case of densely charged IEMs, and as long as the concentration difference across the membrane is

small, that TMS theory predicts the measured membrane potential very well. However, when the concentration difference increases, the unmodified TMS theory starts to deviate from the data. We find that using the ion activity instead of the ion concentration of the solutions adjacent to the membrane leads to a better prediction of the membrane potential. Charge inhomogeneity (charge distribution) has no effect on the membrane potential under zero current conditions. The effect of the two stagnant diffusion layers on either side of the membrane is large, but by itself cannot explain the deviation between theory and data. Lowering the effective membrane charge density can improve the theoretical prediction to some extent, but there is no good physical justification for this adjustment. The effect of water transport (osmosis) is small, even when in the theory the membrane-water friction is set to a very low value. Consideration of differences in the ionic mobility of the ions in the membrane phase can have a large effect on the membrane potential and can, just as including the SDLs, help to explain the development of a maximum in the membrane potential.

Acknowledgements

This work was performed in the cooperation framework of Wetsus, European Centre of Excellence for Sustainable Water Technology (www.wetsus.nl). Wetsus is co-funded by the Dutch Ministry of Economic Affairs and Ministry of Infrastructure and Environment, the European Union Regional Development Fund, the Province of Fryslân and the Northern Netherlands Provinces. The authors like to thank the participants of the research theme "Salt" for the fruitful discussions and their financial support. The authors thank J. de Valença (Wetsus) for discussions concerning the TMS theory and help with part of the theory.

Appendix A

In this Appendix we show how the TMS theory can be derived from the Nernst-Planck flux equation which is Eq. (9) in the main text, and here given as Eq. (A1). According to the TMS theory, the membrane potential is the sum of two Donnan potentials and a diffusion potential (Eq. (15)). These two terms will be discussed in this Appendix.

Donnan potential at membrane-solution interface

The Nernst-Planck flux equation describes ion movement as function of a concentration gradient and an electric field gradient, neglecting a convective contribution due to fluid transport,

$$J_i = -D_i\left[\frac{dc_i(x)}{dx} + c_i(x)z_i\frac{d\psi}{dx}\right] \tag{A1}$$

where J_i is the ion molar flux, $\psi=\phi/VT$ is the dimensionless electrical potential, and D_i is the ion diffusion coefficient. The thermal voltage VT is given by $VT=RT/F$.

To derive the Donnan potential, Eq. (A1) is solved for the case that the gradients are much larger than the ion flux, which results in

$$\frac{1}{c_i}\frac{\partial c_i}{\partial x} = -z_i\frac{\partial\psi}{\partial x} \tag{A2}$$

Next, Eq. (A2) is integrated across the solution-membrane interface, from just outside to just inside the membrane. The resulting voltage difference across the interface is the Donnan potential,

$$\int_{sol}^{mem}\partial\ln c_i = -z_i\int_{sol}^{mem}\partial\psi \tag{A3}$$

$$\ln\frac{c_i^{mem}}{c_i^{sol}} = -z_i(\psi^{mem}-\psi^{sol}) = -z_i\Delta\psi_D \tag{A4}$$

$$c_i^{mem} = c_i^{sol}\exp\left(-z_i\Delta\psi\right) \tag{A5}$$

Both in the external solution, Eq. (A6), and in the membrane phase, Eq. (A7), electroneutrality is assumed, which is given for a 1:1 salt as

$$c_+ - c_- = 0 \tag{A6}$$

$$\overline{c_+} - \overline{c_-} + \omega X = 0 \tag{A7}$$

where the overbar refers to ion concentrations in the membrane. The fixed membrane charge density, X, is defined as a positive number while the charge sign, ω, is either -1 (for CEM) or +1 (for AEM). Combining Eqs. (A5)-(A7) results in

$$2c^{sol}\sinh\left(\Delta\psi_D\right) = \omega X \tag{A8}$$

To obtain an expression for the Donnan potential on either solution-membrane interphase the equation can be rewritten as

$$\Delta\psi_D^{L,R} = \omega\cdot\ln\left[\frac{1}{c_{L,R}^{sol}}\left(X+\sqrt{X^2+(2c_{L,R}^{sol})^2}\right)\right] \tag{A9}$$

Because two Donnan potentials develop, one on left side (L) of the membrane and one on the right side (R), the total Donnan potential is then given as

$$\Delta\psi_D = \omega\cdot\ln\left[\frac{c_R^{sol}}{c_L^{sol}}\frac{\left(X+\sqrt{X^2+(2c_L^{sol})^2}\right)}{\left(X+\sqrt{X^2+(2c_R^{sol})^2}\right)}\right] \tag{A10}$$

Diffusion potential (potential difference within membrane)

Due to the imperfect selectivity of the IEMs a small number of co-ions will diffuse through the membrane from the high concentration side to the low concentration side. For zero-current conditions, this co-ion flux is the same as the counterion flux. The current, being zero, is given by

$$J_+ - J_- = -\overline{D_+}\left(\frac{\partial\overline{c_+}}{\partial x} + \overline{c_+}\frac{\partial\psi}{\partial x}\right) + \overline{D_-}\left(\frac{\partial\overline{c_-}}{\partial x} - \overline{c_-}\frac{\partial\psi}{\partial x}\right) = 0 \tag{A11}$$

For further simplification, we divide by the diffusion coefficient of the positive ion, so there is only one system parameter, α,

$$\alpha = \frac{\overline{D_-}}{\overline{D_+}} \tag{A12}$$

and Eq. (A7) is used to relate the counterions to co-ions, to result in

$$-\left(\frac{\partial\overline{c_+}}{\partial x} + \overline{c_+}\frac{\partial\psi}{\partial x}\right) + \alpha\left(\frac{\partial\left(\overline{c_+}+\omega X\right)}{\partial x} - \left(\overline{c_+}+\omega X\right)\frac{\partial\psi}{\partial x}\right) = 0 \tag{A13}$$

The membrane charge is assumed to be homogenously distributed and therefore, X is independent of x, and the variables can be separated, resulting in

$$\frac{\partial\psi}{\partial x} = \frac{(\alpha-1)}{\alpha\omega X + (\alpha+1)\overline{c_+}}\frac{\partial\overline{c_+}}{\partial x} \tag{A14}$$

which can be integrated across the membrane, leading to

$$\psi_{diff} = \frac{(\alpha-1)}{(\alpha+1)}\ln\frac{\alpha\omega X + (\alpha+1)\overline{c_+^R}}{\alpha\omega X + (\alpha+1)\overline{c_+^L}} \tag{A15}$$

At the solution-membrane interfaces on the left hand and right hand side of the membrane, the expressions for the Donnan equilibrium can be used to relate the internal ion concentration to the external concentration and the fixed membrane charge, according to

$$\overline{c_{L,R}} = \frac{1}{2}\sqrt{X^2 + (2c_{L,R})^2} - \frac{1}{2}\omega X \tag{A16}$$

Inserting Eq. (A16) into Eq. (A15) leads to the following expression of the (dimensionless) diffusion potential

$$\psi_{diff} = \frac{(\alpha-1)}{(\alpha+1)}\ln\left[\frac{\frac{(\alpha-1)}{(\alpha+1)}\omega X + \sqrt{X^2 + (2c_R)^2}}{\frac{(\alpha-1)}{(\alpha+1)}\omega X + \sqrt{X^2 + (2c_L)^2}}\right] \tag{A17}$$

Now, the following replacement can be made,

$$\overline{U} = -\frac{(\alpha-1)}{(\alpha+1)} = \frac{\overline{D_+} - \overline{D_-}}{D_+ + D_-} \tag{A18}$$

which can be inserted in Eq. (A17), to obtain

$$\psi_{diff} = \overline{U}\cdot\ln\left[\frac{-\overline{U}\omega X + \sqrt{X^2 + 4c_L}}{-\overline{U}\omega X + \sqrt{X^2 + 4c_R}}\right] \tag{A19}$$

Inserting Eq. (A10) and Eq. (A19) into Eq. (15), leads to the TMS equation,

$$\phi_m/V_T = (\Delta\phi_D + \phi_{diff})/V_T = \omega\ln\frac{c_R}{c_L}\left[\frac{X + \sqrt{X^2 + 4c_L}}{X + \sqrt{X^2 + 4c_R}}\right] + \overline{U}\ln\left[\frac{-\overline{U}\omega X + \sqrt{X^2 + 4c_L}}{-\overline{U}\omega X + \sqrt{X^2 + 4c_R}}\right] \tag{A20}$$

Nomenclature

a_i	ion activity (mol/m^3)
c	ion concentration (mol/m^3)
D	diffusion coefficient (m^2/s)
F	Faraday constant (C/mol)
$f_m\delta$	water-membrane friction coefficient (mol s/m^4)
Ji	ion molar flux (mol/m^2 s)
K_{ij}	coupling coefficient (-)
P	pressure (Pa)
P_i	ion specific permeability (m/s)
u_i	electric mobility (m^2/V s)
R	gas constant (J/mol K)
r_p	pore radius (m)
T	temperature (K)
v_f	fluid velocity (m/s)
X	fixed membrane charge density per unit aqueous phase in membrane (mol/m^3)
x	distance perpendicular to the membrane (m)
z	valence (-)
α	system parameter (-)
β_i	ion partition coefficient (-)
γ_i	activity coefficient (-)
$\Delta\phi_D$	Donnan potential (V)
δ	thickness (m)
λ_D	Debye length (m)
μ	chemical potential (J/mol)
$\tilde{\mu}$	electrochemical potential (J/mol)
Π	osmotic pressure (Pa)
ϕ	electrical potential (V)
ω	indicator for charge sign (-)

The overbar refers to membrane phase (e.g. $\overline{c}$)

References

[1] H. Strathmann, Electrodialysis, a mature technology with a multitude of new applications, Desalination, 264 (2010) 268-288.
[2] R.E. Pattle, Production of electric power by mixing fresh and salt water in the hydroelectric pile, Nature, 174 (1954) 660.
[3] J.W. Post, H.V.M. Hamelers, C.J.N. Buisman, Energy recovery from controlled mixing salt and fresh water with a reverse electrodialysis system, Environ Sci Technol, 42 (2008) 5785-5790.
[4] S. Porada, R. Zhao, A. Van Der Wal, V. Presser, P.M. Biesheuvel, Review on the Science and Technology of Water Desalination by Capacitive Deionization, Prog Mater Sci, 58 (2013) 1388-1442.
[5] B. Sales, M. Saakes, J.W. Post, C.J.N. Buisman, P.M. Biesheuvel, H.V.M. Hamelers, Direct power production from a water salinity difference in a membrane-modified supercapacitor flow cell, Environ Sci Technol, 44 (2010) 5661-5665.
[6] M. Levin, Molecular bioelectricity in developmental biology: new tools and recent discoveries, Bioessays, 34 (2012) 205-217.
[7] M. Yang, W.J. Brackenbury, Membrane potential and cancer progression, Front Physiol, 4 (2013) 185.
[8] L. Pardo, C. Contreras-Jurado, M. Zientkowska, F. Alves, W. Stühmer, Role of voltage-gated potassium channels in cancer, J Membrane Biol, 205 (2005) 115-124.
[9] W. Ostwald, Elektrische Eigenschaften halbdurchlässiger Scheidewände, Z Phys Chem, 6 (1890) 71-82.
[10] F.G. Donnan, Theorie der Membrangleichgewichte und Membranpotentiale bei vorhandensein von nicht dialysierenden elektrolyten. Ein beitrag zur Physikalisch-chemischen Physiologie., Z Elektrochem, 17 (1911) 572-581.
[11] T. Teorell, An Attempt to Formulate a Quantitative Theory of Membrane Permeability Proc Soc Exp Biol Med, 33 (1935) 282-285.
[12] K.H. Meyer, J.F. Sievers, La perméabilité des membranes I. Théorie de la perméabilité ionique, Helv Chim Acta, 19 (1936) 649-664.
[13] A. Staverman, Non-equilibrium thermodynamics of membrane processes, T Faraday Soc, 48 (1952) 176-185.
[14] K.S. Spiegler, Transport processes in ionic membranes, T Faraday Soc, 54 (1958) 1408-1428.
[15] R. Schlögl, Stofftransport durch Membranen, Dr. Dietrich Steinkopff Verlag, Darmstadt, 1964. [16] J.V. Leyendekkers, The chemical potentials of seawater components, Mar Chem, 1 (1973) 75-88.
[17] M. Whitfield, An improved specific interaction model for seawater at 25°C and 1 atmosphere total pressure, Mar Chem, 3 (1975) 197-213.
[18] M. Higa, A. Tanioka, K. Miyasaka, Simulation of the transport of ions against their concentration gradient across charged membranes, J Mem Sci, 37 (1988) 251-266.
[19] T. Teorell, Studies on the "diffusion effect" upon ionic distribution. I. Some theoretical considerations, Proc Natl Acad Sci Wash, 21 (1935) 152-161.
[20] J.R. Wilson, Demineralization by electrodialysis, 1st Ed., Butterworths Scientific Publications, London , 1960.
[21] A.H. Galama, M. Saakes, H. Bruning, H.H.M. Rijnaarts, J.W. Post, Seawater Predesalination with Electrodialysis, Desalination, 342 (2013) 61-69.
[22] F.G. Helfferich, Ion Exchange,1st Ed., McGraw-Hill, New York, (1962).
[23] N. Lakshminarayanaiah, Transport phenomena in membranes, 1st Ed., Academic Press, Philadelphia, 1969.
[24] H. Strathmann, Ion-exchange membrane separation processes, Elsevier, 1st Ed., Amsterdam , 2004.
[25] S. Mafé, V.M. Aguilella, J. Pellicer, Film control and membrane control in charged membranes, J Mem Sci, 36 (1988) 497-509.
[26] R. Schlögl, F.G. Helfferich, Zur Theorie des Potentials von Austascher-Membranen, Z Elektrochem, 56 (1952) 644-647.
[27] T. Teorell, Transport processes and electrical phenomena in ionic membranes, in: J.A. Butler, J.T. Randall, (Eds.), Prog Biophys Biop Ch, Academic Press, New York, 1953, pp. 305-369.
[28] F.G. Donnan, The theory of membrane equilibria, Chem Rev, 1 (1924) 73-90.
[29] K. Sollner, Recent advances in the electrochemistry of membranes of high ionic selectivity, J Electrochem Soc, 97 (1950) 139C-151C.
[30] C. Marshall, The electrochemical properties of mineral membranes. VIII. The theory of selective membrane behavior, J Phys Chem, 52 (1948) 1284-1295.
[31] A. Einstein, Über die von der molekularkinetschen Theorie der Wärme geforderte Bewegung von in ruhenden Flüssigkeiten suspendierten Teilchen, Ann Phys, 322 (1905) 549-560.
[32] M. von Smoluchowski, Zur kinetischen Theorie der Brownschen Molekularbewegung und der Suspensionen, Ann Phys, 326 (1906) 756-780.
[33] W.E. Morf, Calculation of liquid-junction potentials and membrane potentials on the basis of the planck theory, Anal Chem, 49 (1977) 810-813.
[34] D.E. Goldman, Potential, Impedance, and Rectification in Membranes, J Gen Physiol, 27 (1943) 37-60.
[35] W.F. Pickard, Generalizations of the Goldman-Hodgkin-Katz equation, Math Biosci, 30 (1976) 99-111.
[36] P. Moon, G. Sandí, D. Stevens, R. Kizilel, Computational modeling of ionic transport in continuous and batch electrodialysis, Sep Sci Technol, 39 (2004) 2531-2555.
[37] Y. Kim, W.S. Walker, D.F. Lawler, Competitive separation of di- vs. mono-valent cations in electrodialysis: Effects of the boundary layer properties, Water Res, 46 (2012) 2042-2056.
[38] Y. Tanaka, Concentration polarization in ion-exchange membrane electrodialysis—the events arising in a flowing solution in a desalting cell, J Mem Sci, 216 (2003) 149-164.
[39] C. Forgacs, N. Ishibashi, J. Leibovitz, J. Sinkovic, K.S. Spiegler, Polarization at ion-exchange membranes in electrodialysis, Desalination, 10 (1972) 181-214.
[40] P.M. Biesheuvel, Two-fluid model for the simultaneous flow of colloids and fluids in porous media, J Colloid Interf Sci, 355 (2011) 389-395.
[41] R.B. Gunn, P.F. Curran, Membrane potentials and ion permeability in a cation exchange membrane, Biophys J, 11 (1971) 559-571.
[42] A.L. Hodgkin, B. Katz, The effect of sodium ions on the electrical activity of the giant axon of the squid, J Physiol, 108 (1949) 37-77.
[43] T. Sata, Ion Exchange Membranes; Preparation, Characterization, Modification and Application, 1st Ed., The Royal Society of Chemistry, Cambridge , 2004.

[44] A.H. Galama, J.W. Post, M.A. Cohen Stuart, P.M. Biesheuvel, Validity of the Boltzmann equation to describe Donnan equilibrium at the membrane-solution interface, J Mem Sci, 442 (2013) 131-139.
[45] T. Xu, Ion exchange membranes: State of their development and perspective, J Mem Sci, 263 (2005) 1-29.
[46] H.P. Gregor, Gibbs-donnan equilibria in ion exchange resin systems, J Am Chem Soc, 73 (1951) 642-650.
[47] E. Glueckauf, R.E. Watts, The Donnan law and its application to ion exchanger polymers, Proc Roy Soc A, 269 (1962) 339-349.
[48] K. Kontturi, L. Murtomäki, J.A. Manzanares, Ionic Transport Processes: in Electrochemistry and Membrane Science, 1st Ed., Oxford University Press, New York, 2008.
[49] G.B. Westermann-Clark, C.C. Christoforou, The exclusion-diffusion potential in charged porous membranes, J Electroanal Chem, 198 (1986) 213-231.
[50] Y. Oren, A. Litan, The state of the solution-membrane interface during ion transport across an ion-exchange membrane, J Phys Chem, 78 (1974) 1805-1811.
[51] K.N. Mikhelson, A. Lewenstam, S.E. Didina, Contribution of the diffusion potential to the membrane potential and to the ion-selective electrode response, Electroanal, 11 (1999) 793-798.
[52] B. Auclair, V. Nikonenko, C. Larchet, M. Métayer, L. Dammak, Correlation between transport parameters of ion-exchange membranes, J Mem Sci, 195 (2002) 89-102.
[53] Y. Lanteri, A. Szymczyk, P. Fievet, Membrane potential in multi-ionic mixtures, J Phys Chem B, 113 (2009) 9197-9204.
[54] Y. Lanteri, A. Szymczyk, P. Fievet, Influence of steric, electric, and dielectric effects on membrane potential, Langmuir, 24 (2008) 7955-7962.
[55] K. Asaka, Electrochemical properties of asymmetric cellulose acetate membranes, J Mem Sci, 52 (1990) 57-76.
[56] M. Ersoz, The electrochemical properties of polysulfone ion-exchange membranes, J Colloid Interf Sci, 243 (2001) 420-426.
[57] W.J. Shang, X.L. Wang, Y.X. Yu, Theoretical calculation on the membrane potential of charged porous membranes in 1-1, 1-2, 2-1 and 2-2 electrolyte solutions, J Mem Sci, 285 (2006) 362-375.
[58] Y. Kobatake, N. Takeguchi, Y. Toyoshima, H. Fujita, Studies of membrane phenomena. I. Membrane potential, J Phys Chem, 69 (1965) 3981-3988.
[59] M. Kawaguchi, T. Murata, A. Tanioka, Membrane potentials in charged membranes separating solutions of weak electrolytes, J Chem Soc Faraday Trans, 93 (1997) 1351-1356.
[60] M. Tasaka, N. Aoki, Y. Kondo, M. Nagasawa, Membrane potentials and electrolyte permeation velocities in charged membranes, J Phys Chem, 79 (1975) 1307-1314.
[61] A.H. Galama, G. Daubaras, O.S. Burheim, H.H.M. Rijnaarts, J.W. Post, Seawater electrodialysis with preferential removal of divalent ions, J Mem Sci, 452 (2014) 219-228.
[62] W. Nernst, Theorie der Reaktionsgeschwindigkeit in heterogenen Systemen, Z phys Chem, 47 (1904) 52-55.
[63] B. Levich, The theory of concentration polarisation, Discuss Faraday Soc, 1 (1947) 37-49.
[64] D. Mackay, P. Meares, On the correction for unstirred solution films in ion-exchange membrane cells, Kolloid Z, 167 (1959) 31-39.
[65] K.S. Spiegler, Polarization at ion exchange membrane-solution interfaces, Desalination, 9 (1971) 367-385.
[66] L. Dammak, C. Larchet, B. Auclair, Theoretical study of the bi-ionic potential and confrontation with experimental results, J Mem Sci, 155 (1999) 193-207.
[67] L. Dammak, C. Larchet, B. Auclair, V. Nikonenko, V. Zabolotsky, From the multi-ionic to the bi-ionic potential, Eur Polym J, 32 (1996) 1199-1205.
[68] E. Kumamoto, Effect of unstirred layers on the membrane potential in a concentration cell, J Mem Sci, 9 (1981) 43-51.
[69] C. Larchet, S. Nouri, B. Auclair, L. Dammak, V. Nikonenko, Application of chronopotentiometry to determine the thickness of diffusion layer adjacent to an ion-exchange membrane under natural convection, Adv Colloid Interf Sci, 139 (2008) 45-61.
[70] J.B. Jensen, T.S. Sørensen, B. Malmgren-Hansen, P. Sloth, Ion exchange and membrane potentials in cellulose acetate membranes separating solutions of mixed electrolytes, J Colloid Interf Sci, 108 (1985) 18-30.
[71] V.M. Barragán, C. Ruíz-Bauzá, Membrane potentials and electrolyte permeation in a cation-exchange membrane, J Mem Sci, 154 (1999) 261-272.
[72] M. Nagasawa, Y. Kobatake, The theory of membrane potential, J Phys Chem, 56 (1952) 1017-1024.
[73] T.S. Sørensen, V. Compañ, Salt flux and electromotive force in concentration cells with asymmetric ion exchange membranes and ideal 2:1 Electrolytes, J Phys Chem, 100 (1996) 15261-15273.
[74] Y. Lanteri, P. Fievet, A. Szymczyk, Evaluation of the steric, electric, and dielectric exclusion model on the basis of salt rejection rate and membrane potential measurements, J Colloid Interf Sci, 331 (2009) 148-155.
[75] X. Lefebvre, J. Palmeri, Nanofiltration theory: Good Co-Ion exclusion approximation for single salts, J Phys Chem B, 109 (2005) 5525-5540.
[76] D. Liu, Y. Zhang, Membrane potentials across the cation exchange membrane in aqueous mixed electrolyte solutions, in: W. Chen, Q. Li, Y. Chen, P. Dai, Z. Jiang (Eds.) Adv Mat Res, 2012, pp. 1825-1828.
[77] C.A. Lewis, Ion-concentration dependence of the reversal potential and the single channel conductance of ion channels at the frog neuromuscular junction, J Physiol, 286 (1979) 417-445.
[78] S.G. Spangler, Expansion of the constant field equation to include both divalent and monovalent ions, Ala J Med Sci, 9 (1972) 218-223.
[79] O. Kedem, A. Katchalsky, A physical interpretation of the phenomenological coefficients of membrane permeability, J Gen Physiol, 45 (1961) 143-179.
[80] O. Kedem, A. Katchalsky, Permeability of composite membranes. Part 1.-Electric current, volume flow and flow of solute through membranes, Trans Faraday Soc, 59 (1963) 1918-1930.
[81] I. Michaeli, O. Kedem, Description of the transport of solvent and ions through membranes in terms of differential coefficients. Part 1.—Phenomenological characterization of flows, Trans Faraday Soc, 57 (1961) 1185-1190.
[82] A. Katchalsky, O. Kedem, Thermodynamics of flow processes in biological systems, Biophys J, 2 (1962) 53-78.
[83] A. Mauro, A. Finkelstein, Realistic model of a fixed-charge membrane according to the theory of Teorell, Meyer, and Sievers, J Gen Physiol, 42 (1958) 385-391.
[84] G.J. Hills, P.W.M. Jacobs, N. Lakshminarayanan, Membrane Potentials I. The Theory of the e.m.f. of cells containing ion- exchange membranes, Proc Roy Soc A, 262 (1961) 246-256.
[85] J. Mackie, P. Meares, The diffusion of electrolytes in a cation-exchange resin membrane. I. Theoretical, P Roy Soc A - Math Phy, 232 (1955) 498-509.
[86] J. Cervera, V. García-Morales, J. Pellicer, Ion size effects on the electrokinetic flow in nanoporous membranes caused by concentration gradients, J Phys Chem B, 107 (2003) 8300-8309.
[87] V.M. Barragán, J.P.G. Villaluenga, M.P. Godino, M.A. Izquierdo-Gil, C. Ruiz-Bauzá, B. Seoane, Experimental estimation of equilibrium and transport properties of sulfonated cation-exchange membranes with different morphologies, J Colloid Interf Sci, 333 (2009) 497-502.
[88] V.M. Barragán, M.J. Pérez-Haro, Correlations between water uptake and effective fixed charge concentration at high univalent electrolyte concentrations in sulfonated polymer cation-exchange membranes with different morphology, Electrochim Acta, 56 (2011) 8630-8637.
[89] E. Fetcher Jr, A Criticism of the Teorell–Meyer–Sievers Theory of Membrane Permeability, J Phys Chem, 46 (1942) 570-574.
[90] A. Sonin, Osmosis and Ion Transport in Charged Porous Membranes: A Macroscopic, Mechanistic Model, in: E. Sélégny, G. Boyd, H. Gregor (Eds.) Charged Gels and Membranes, Springer Netherlands, 1976, pp. 255-265.
[91] W.B.S. de Lint, P.M. Biesheuvel, H. Verweij, Application of the charge regulation model to transport of ions through hydrophilic membranes: one-dimensional transport model for narrow pores (nanofiltration), J Colloid Interf Sci, 251 (2002) 131-142.
[92] R. Schlögl, The significance of convection in transport processes across porous membranes, Discuss Faraday Soc, 21 (1956) 46-52.
[93] F.A. Morrison Jr, J.F. Osterle, Electrokinetic energy conversion in ultrafine capillaries, J Chem Phys, 43 (1965) 2111-2115.
[94] R.J. Gross, J.F. Osterle, Membrane transport characteristics of ultrafine capillaries, J Chem Phys, 49 (1968) 228-234.
[95] J.C. Fair, J.F. Osterle, Reverse electrodialysis in charged capillary membranes, J Chem Phys, 54 (1971) 3307-3316.
[96] V. Sasidhar, E. Ruckenstein, Electrolyte osmosis through capillaries, J Colloid and Interf Sci, 82 (1981) 439-457.
[97] G.B. Westermann-Clark, J.L. Anderson, Experimental verification of the space-charge model for electrokinetics in charged microporous membranes, J Electrochem Soc, 130 (1983) 839-847.
[98] L. Onsager, R.M. Fuoss, Irreversible processes in electrolytes. Diffusion, conductance, and viscous flow in arbitrary mixtures of strong electrolytes, J Phys Chem, 36 (1932) 2689-2778.
[99] A. Mauro, Nature of solvent transfer in osmosis, Science, 126 (1957) 252-253.
[100] P.M. Ray, On the theory of osmotic water movement, Plant physiol, 35 (1960) 783-795.
[101] R. Schlögl, Theory of anomalous osmosis, Z Phys Chem NF, 3 (1955) 73-102.
[102] J.L. Anderson, D.M. Malone, Mechanism of osmotic flow in porous membranes, Biophys J, 14 (1974) 957-982.
[103] I. Medved, R. Černý, Osmosis in porous media: A review of recent studies, Micropor Mesopor Mat, 170 (2013) 299-317.
[104] A. Yaroshchuk, Osmosis and reverse osmosis in fine-porous charged diaphragms and membranes, Adv Colloid Interf Sci, 60 (1995) 1-93.
[105] N. Lakshminarayanaiah, Electroosmosis in Ion-Exchange Membranes, J Electrochem Soc, 116 (1969) 338-343.
[106] N.P. Berezina, S.A. Shkirskaya, A.A.R. Sycheva, M.V. Krishtopa, The electric transport of proton-bound water in MF-4SK/PAni nanocomposite membranes, Colloid J, 70 (2008) 397-406.
[107] J. Barrett, Inorganic chemistry in aqueous solution, in: E.W. Abel (Ed.), Royal Society of Chemistry, Cambridge , 2003.
[108] B. Tansel, J. Sager, T. Rector, J. Garland, R.F. Strayer, L. Levine, M. Roberts, M. Hummerick, J. Bauer, Significance of hydrated radius and hydration shells on ionic permeability during nanofiltration in dead end and cross flow modes, Sep Purif Technol, 51 (2006) 40-47.
[109] V.I. Zabolotskii, O.A. Demina, K.V. Protasov, Capillary model of electroosmotic transport of the free solvent through ion-exchange membranes, Russ J Electrochem, 50 (2014) 412-418.
[110] V.I. Zabolotskii, K.V. Protasov, M.V. Sharafan, Sodium chloride concentration by electrodialysis with hybrid organic-inorganic ion-exchange membranes: An investigation of the process, Russ J Electrochem, 46 (2010) 979-986.
[111] N.P. Berezina, E.N. Komkova, A comparative study of the electric transport of ions and water in sulfonated cation-exchange polymeric membranes of the new generation, Kolloidnyj Z, 65 (2003) 5-15.
[112] Y. Kobatake, Y. Toyoshima, N. Takeguchi, Studies of membrane phenomena. II. Theoretical study of membrane potentials, J Phys Chem, 70 (1966) 1187-1193.
[113] P.M. Biesheuvel, S. Porada, M. Levi, M.Z. Bazant, Attractive forces in microporous carbon electrodes for capacitive deionization, J Solid State Electr, 18 (2014) 1365-1376.
[114] A. Yaroshchuk, Current-induced concentration polarization of interfaces between non-ideally perm-selective ion-exchange media and electrolyte solutions, J Mem Sci, 396 (2012) 43-49.
[115] J.A. Manzanares, S. Mafé, J. Bisquert, Electric Double Layer at the Membrane/Solution Interface: Distribution of Electric Potential and Estimation of the Charge Stored, Ber Bunsen Gesell, 96 (1992) 538-544.
[116] J. Kielland, Individual activity coefficients of ions in aqueous solutions, J Am Chem Soc, 59 (1937) 1675-1678.
[117] A. Volkov, S. Paula, D. Deamer, Two mechanisms of permeation of small neutral molecules and hydrated ions across phospholipid bilayers, Bioelectroch Bioenerg, 42 (1997) 153-160.
[118] J. Cervera, P. Ramírez, J.A. Manzanares, S. Mafé, Incorporating ionic size in the transport equations for charged nanopores, Microfluid Nanofluid, 9 (2010) 41-53.
[119] O. Stern, Zur Theorie der Elektrolytischen Doppelschicht, Z Elektrochem Angew P, 30 (1924) 508-516.
[120] L.L. Zhang, X.S. Zhao, Carbon-based materials as supercapacitor electrodes, Chem Soc Rev, 38 (2009) 2520-2531.
[121] J.C. Eijkel, A. van den Berg, Nanofluidics and the chemical potential applied to solvent and solute transport, Chem Soc Rev, 39 (2010) 957-973.
[122] S. Basu, M.M. Sharma, An improved Space-Charge model for flow through charged microporous membranes, J Mem Sci, 124 (1997) 77-91.
[123] P. Długołęcki, K. Nymeijer, S. Metz, M. Wessling, Current status of ion exchange membranes for power generation from salinity gradients, J Mem Sci, 319 (2008) 214-222.
[124] A.H. Galama, D.A. Vermaas, J. Veerman, M. Saakes, H.H.M. Rijnaarts, J.W. Post, K. Nijmeijer, Membrane resistance: The effect of salinity gradients over a cation exchange membrane, J Mem Sci, 467 (2014) 279-291.
[125] Y. Kobatake, N. Kamo, Transport processes in charged membranes, Prog Polymer Sci Jap, 5 (1973) 257.
[126] CRC Handbook of Chemistry and Physics, 85th Ed., Boca Raton, Florida, 2004.
[127] C. Marshall, W. Bergman, The Electrochemical Properties of Mineral Membranes. I. The Estimation of Potassium Ion Activities*, J Am Chem Soc, 63 (1941) 1911-1916.
[128] S. Mafé, P. Ramírez, J. Pellicer, Activity coefficients and Donnan coion exclusion in charged membranes with weak-acid fixed charge groups, J Mem Sci, 138 (1998) 269-277.

[129] E.H. Cwirko, R.G. Carbonell, Ionic equilibria in ion-exchange membranes: a comparison of pore model predictions with experimental results, J Mem Sci, 67 (1992) 211-226.
[130] E. Glueckauf, A New Approach to Ion Exchange Polymers, Proc Roy Soc A, 268 (1962) 350-370.
[131] P. Ramírez, V. Gómez, J. Cervera, B. Schiedt, S. Mafé, Ion transport and selectivity in nanopores with spatially inhomogeneous fixed charge distributions, J Chem Phys, 126 (2007) 194703.
[132] J.A. Manzanares, S. Mafe, J. Pellicer, Transport phenomena and asymmetry effects in membranes with asymmetric fixed charge distributions, J Phys Chem, 95 (1991) 5620-5624.
[133] A. Genç, Membrane potentials for linearly varying fixed charges, Turk J Eng Env Sci, 33 (2009) 73-81.
[134] S. Ohki, Electrical potential of an asymmetric membrane, J Colloid Interf Sci, 37 (1971) 318-324.
[135] N. Kamo, Y. Kobatake, Interpretation of asymmetric membrane potential, J Colloid and Interf Sci, 46 (1974) 85-93.
[136] R. Takagi, M. Nakagaki, Facilitated and reverse transport of electrolytes through an asymmetric membrane, J Mem Sci, 27 (1986) 285-299.
[137] A.V. Sokirko, J.A. Manzanares, J. Pellicer, The Permselectivity of Membrane Systems with an Inhomogeneous Distribution of Fixed Charge Groups, J Colloid Interf Sci, 168 (1994) 32-39.
[138] M. Nishizawa, V.P. Menon, C.R. Martin, Metal Nanotubule Membranes with Electrochemically Switchable Ion-Transport Selectivity, Science, 268 (1995) 700-702.
[139] J. Mayer, K. Khairy, J. Howard, Drawing an elephant with four complex parameters, Am J Phys, 78 (2010) 648.
[140] R. Yamamoto, H. Matsumoto, A. Tanioka, Ionic transport behavior across charged membranes with low water content. I. Theoretical aspect of membrane potentials in membranes having inhomogeneously distributed fixed-charge groups, J Phys Chem B, 107 (2003) 10615-10622.
[141] A.A. Qaiser, M.M. Hyland, D.A. Patterson, Membrane potential and impedance studies of polyaniline composite membranes: Effects of membrane morphology, J Mem Sci, 385 (2011) 67-75.
[142] I. Makra, G. Jágerszki, I. Bitter, R.E. Gyurcsányi, Nernst–Planck/Poisson model for the potential response of permselective gold nanopores, Electrochim Acta, 73 (2012) 70-77.
[143] P. Bühlmann, S. Amemiya, S. Yajima, Y. Umezawa, Co-Ion Interference for Ion-Selective Electrodes Based on Charged and Neutral Ionophores: A Comparison, Anal Chem, 70 (1998) 4291-4303.
[144] M. Tasaka, S. Morita, M. Nagasawa, Membrane potential in nonisothermal systems, J Phys Chem, 69 (1965) 4191-4197.
[145] M. Tasaka, T. Mizuta, O. Sekiguchi, Mass transfer through polymer membranes due to a temperature gradient, J Mem Sci, 54 (1990) 191-204.
[146] S. Kim, M. Mench, Investigation of temperature-driven water transport in polymer electrolyte fuel cell: Thermo-osmosis in membranes, J Mem Sci, 328 (2009) 113-120.
[147] P. Biesheuvel, D. Brogioli, H. Hamelers, Negative Joule Heating in Ion-Exchange Membranes, preprint arXiv:1402.1448, (2014).